



**HAL**  
open science

# IGNSS Computation Models and Values for GPS and GALILEO Civil Aviation Receivers

Axel Javier Garcia Peña, Christophe Macabiau, Olivier Julien, Mikael Mabillean, Pierre Durel

► **To cite this version:**

Axel Javier Garcia Peña, Christophe Macabiau, Olivier Julien, Mikael Mabillean, Pierre Durel. IGNSS Computation Models and Values for GPS and GALILEO Civil Aviation Receivers. ION GNSS+ 2020, 33rd International Technical Meeting of the Satellite Division of the Institute of Navigation, Sep 2020, Virtual event, United States. pp 206 - 218, 10.33012/2020.17571 . hal-02964000

**HAL Id: hal-02964000**

**<https://enac.hal.science/hal-02964000>**

Submitted on 9 May 2022

**HAL** is a multi-disciplinary open access archive for the deposit and dissemination of scientific research documents, whether they are published or not. The documents may come from teaching and research institutions in France or abroad, or from public or private research centers.

L'archive ouverte pluridisciplinaire **HAL**, est destinée au dépôt et à la diffusion de documents scientifiques de niveau recherche, publiés ou non, émanant des établissements d'enseignement et de recherche français ou étrangers, des laboratoires publics ou privés.

# $I_{GNSS}$ Computation Models and Values for GPS and GALILEO L5/E5a Civil Aviation Receivers

**Axel Garcia-Pena, Christophe Macabiau, Ecole Nationale de l'Aviation Civile (ENAC)**

**Olivier Julien, U-blox**

**Mikael Mabilieu, Pierre Durel, European GNSS Agency (GSA)**

## BIOGRAPHIES

Axel GARCIA-PENA is a researcher/lecturer with the SIGnal processing and NAVigation (SIGNAV) research axis of the TELECOM lab of ENAC (French Civil Aviation University), Toulouse, France. His research interests are GNSS navigation message demodulation, optimization and design, GNSS receiver design and GNSS satellite payload. He received his double engineer degree in 2006 in digital communications from SUPAERO and UPC, and his PhD in 2010 from the Department of Mathematics, Computer Science and Telecommunications of the INPT (Polytechnic National Institute of Toulouse), France.

Christophe MACABIAU is Christophe Macabiau graduated as an electronics engineer in 1992 from the ENAC (Ecole Nationale de l'Aviation Civile) in Toulouse, France. Since 1994, he has been working on the application of satellite navigation techniques to civil aviation. He received his Ph.D in 1997 and has been in charge of the signal processing lab of ENAC since 2000, where he also started dealing with navigation techniques for terrestrial navigation. He is currently the head of the TELECOM team of ENAC, that includes research groups on signal processing and navigation, electromagnetics, and data communication networks.

Olivier JULIEN is a Senior Principal Engineer in u-blox AG, Switzerland since December 2018. He was the head of the Signal Processing and Navigation (SIGNAV) research group of the TELECOM laboratory of ENAC, in Toulouse, France. He received his engineer degree in 2001 in digital communications from ENAC and his PhD in 2005 from the Department of Geomatics Engineering of the University of Calgary, Canada. His research interests are turned towards the use of satellite-based navigation systems for safe navigation.

Mikael MABILLEAU is a standardisation engineer on SBAS in the EGNOS exploitation team of the European GNSS Agency (GSA). Since his graduation as engineer from the French civil aviation school (ENAC) in 2006, he has been involved in GNSS standardization activity carried by the main civil aviation standardisation bodies such as the EUROCAE WG 62 on Galileo, RTCA Special Committee 159 on GPS and the International Civil Aviation Organisation (ICAO) Navigation System Panel in charge of ICAO standard. Mikael is involved in the evolution of GNSS concepts (ARAIM and SBAS L1L5) supporting the development of the associated standards (SARPs and MOPS) for use in aviation.

Pierre DUREL graduated in 2002 from the University of Montpellier II as an engineer specialized in hyper-frequencies and optronics. He is working as EGNOS Services Engineer for the European GNSS Agency. He is involved in standardization activities dealing with DFMC SBAS for which he is secretary of EUROCAE Galileo Working Group 62.

## ABSTRACT

GNSS L5/E5a interference environment is dominated by DME/TACAN and JTIDS/MIDS pulses causing a degradation of the effective  $C/N_0$  observed by the receiver. A time-domain blanker is implemented to mitigate their impact. RTCA DO-292 proposes a model to compute the  $C/N_0$  degradation of the received useful signal by the increase of the noise PSD.

This paper focuses on the computation on the max value of the  $I_{GNSS}$  term.

## INTRODUCTION

Processing of GNSS received signals can be affected by received additive signals such as noise, multipath and interference. Radio Frequency Interference (RFI) sources are of various sorts and their nature and impact depends on the user application. In the context of civil aviation, it is important to identify and characterize the radio frequency interference relevant to the airborne GNSS receivers processing signals in the L1/E1 and L5/E5a bands. This characterization serves to determine the degradation of performance of these airborne GNSS receivers in L1/E1 and L5/E5a equipped with their relevant antenna which is then compared to operational

performance thresholds, then serves to issue maximum tolerable levels of aggregate non aeronautical interference in order to protect the spectrum. Finally, this prediction of degradation of performance compared to functional thresholds is used to issue minimum requirements on these L1/E1 and L5/E5a antennas, and to set minimum requirements to be imposed on airborne GNSS receivers operating at L1/E1 and L5/E5a bands. A long thread of activities led to the elaboration of various ICAO, RTCA and EUROCAE standards considering RFI. Currently, [1] reflecting the relevant interference to L5/E5a is being updated to incorporate the evolutions of the RFI environment defined by DME/TACAN, JTIDS/MIDS, LDACS, SSR equipment and other GNSS systems operating at these bands, as well as the usage of this L5/E5a band for GALILEO E5a and SBAS L5/E5a datalink airborne signal processing. In addition, ICAO RFI mask of GNSS L5/E5a is now under definition and validation. These elements will then complement the current ICAO SARPs, draft EUROCAE and RTCA MOPS for GNSS L5/E5a airborne receivers.

In the course of the elaboration of the ICAO SARPs validation and of the update of [1], it has been proposed to revisit several elements of the worst-case link budget analysis in order to consolidate the overall link budget margin. This was deemed necessary since the link budget margin is expected to be small. Among the axes of revision are:

- the analytical model representing the effect of the AGC/ADC and temporal blanker
- the DME/TACAN environment and its impact on a minimum operational/system performance requirements for a GNSS L5/E5a receiver
- the JTIDS/MIDS environment and its impact on a minimum operational/system performance requirements for a GNSS L5/E5a receiver
- The consideration of SSR and LDACS

This article specifically looks at the consolidation of the model of the effect of wideband continuous GNSS interference on a civil aviation airborne GNSS receiver.

The RFI impact on a GNSS receiver in civil aviation is usually modelled as the  $C/N_0$  degradation observed at the receiver's correlator output, or equivalently, as an increase of the effective  $N_0$  denoted as  $N_{0,eff}$ . Therefore, a decrease of the minimum available  $C/N_0$ , derived from the link budget and from the  $N_{0,eff}$  calculation, implies a reduction of the  $C/N_0$  margin between the minimum available  $C/N_{0,eff}$  and the different L5/E5a GNSS and SBAS L5 signal processing, acquisition, tracking, demodulation,  $C/N_0$  threshold values. Concerning the revisit of several elements determining the  $C/N_0$  margin, first, the model for the GNSS airborne receiver RF processing chain, namely the model for AGC/ADC and blanker is reviewed. In particular, the model for blanking function has gone under new scrutiny, with the prospect of the definition of a minimum blanker model. Second, the DME/TACAN environment is being reviewed. Models of impact of DME/TACAN on  $C/N_0$  degradation are also revised. Next, the JTIDS/MIDS environment will be re-assessed, and the relevant models updated. LDACS and SSR will also need to be inspected.

Traditionally, the countermeasure adopted against pulse interference which is analyzed in civil aviation is the temporal domain pulse blanking method as described in [1]. Temporal domain blanking method is easy to implement and computationally efficient. It can thus be considered as representative of what could be implemented in a minimum airborne receiver.

The expression of effective  $N_0$  at the output of the receiver antenna in the presence of non-pulsed and pulsed interference and with a temporal blanker is given below:

$$N_{0,eff} = \frac{N_0}{1-bdc} * \left( 1 + \frac{I_{0,WB}}{N_0} + R_I \right) \quad (1)$$

where  $I_{0,WB}$  are all the wideband (non-pulsed) continuous RFI contributions (usually the other GNSS signals falling in the L5/E5a band). Setting the blanking threshold correctly can be challenging due to the trade-off between the Blanking Duty Cycle, abbreviated as  $bdc$  (percentage of samples set to zero by the blanker) also sometimes called the Pulse Duty Cycle of the blanker abbreviated as  $PDC$  depending on the authors [1], and the  $R_i$  (the below-blanker interfering-signal-to-thermal-noise ratio) parameters since both of them directly impact the effective noise,  $N_0$ , of the received signal after blanking. On one hand, a low threshold removes the majority of the signal samples containing interference because they will exceed the threshold (reduction of  $R_I$ ), but such a low threshold causes that fact a higher percentage of time the noise alone is enough to trigger the zero-setting process causing a "false alarm" (increase of  $bdc$ ), and therefore this setting of samples to 0 due to noise and interference also suppresses the useful GNSS signal energy. On the other hand, a high threshold value decreases the "false alarm" events due to noise and lets some interference and useful GNSS signal energy go through (decrease of  $bdc$ ), but also does not appropriately suppress the interference samples (increase of  $R_I$ ). In the situation of pulsed interference, proper blanker threshold selection is thus the result of a compromise and a crucial factor of performance in such blanking methods.

The interference of concern in this paper is the continuous GNSS interference leading to a contribution called  $I_{GNSS}$  to the  $I_{0,WB}$  mentioned above, due to the inter- and intra- GNSS system interference which is a type of continuous interference. This interference

also has a received power level so low that it never triggers the blanker, although it may be blanked itself due to the presence of other strong pulsed interference.

The general aim of this paper is thus to present ways to compute the specific efficient  $N_{0,eff}$  degradation using the general methodology to assess the effect of the different GNSS interference sources on the increase of the background noise for GPS L1, GALILEO E1 OS, Galileo E5a or GPS L5 signals in presence of GNSS only as interference sources. The specific objectives of this paper can be listed as follows:

1. Introduce the model for the civil aviation GNSS L5/E5a receiver
2. Present the model for  $N_{0,eff}$  and  $R_I$  involving SSCs
3. Present model for  $I_{GNSS}$
4. Present GNSS satellites and user receiver antenna assumptions
5. Present GNSS constellations assumptions
6. Present GNSS signals assumptions
7. Present results of  $I_{GNSS}$  for GPS L5, GALILEO E5a BPSK 10
8. Draw new conclusions on the modeling of the effect of continuous GNSS interference which can be further recommended in ICAO SARPs and EUROCAE/RTCA MOPS development

### 1) MODEL FOR GNSS L5/E5A CIVIL AVIATION RECEIVER

DME, and its military equivalent, TACAN, are two systems used by aircraft to know their distance to a ground station, which position is known. The systems operate as follows: the aircraft DME equipment (called interrogator) sends pulses to ground stations. Once the interrogation is detected, the station transponder replies to the interrogator. The distance is then determined by the aircraft interrogator by measuring the time elapsed between each pulse transmitted by the interrogator and the reception of its corresponding reply pulse from the transponder. This time corresponds to twice the distance between the aircraft and the station, plus fixed processing time inside the ground station.

According to [1], only the signals emitted in the band of interest of the study disturb GNSS receivers operations. Indeed, the band of interest is the E5a/L5 one and equals [1164 MHz; 1191 MHz], The aircraft’s DME interrogators emitting their signals between 1025 and 1151 MHz or between 1191 MHz and 1215 MHz are ignored herein.

The main on-board signal representing a risk for E5a/L5 is transmitted by the DME interrogator. Indeed the nearest airborne channel is 26.45 MHz below E5a/L5. Although the produced pulses are highly spectrally constrained and attenuated at this central frequency by the RF Front-End, they could produce saturation at E5a/L5 stretching the pulses duration, but their impact is constrained to  $bdc_{DME/TACAN\_airborne} = 0.0026$  and  $R_{I,DME/TACAN\_airborne}=0.002$ . Interrogators from nearby aircraft were shown to induce a negligible impact [1].

The study therefore focuses on DME ground stations, as they emit their signals between 962 and 1213 MHz, which includes the above defined band of interest. The only ground DME beacons of interest in this analysis are the beacons operating in X mode, for which the central frequency is larger or equal to 1151 MHz.

The Joint Tactical Information Distribution System (JTIDS) and the Multifunctional Information Distribution System (MIDS) are military aeronautical digital tactical communication, navigation and identification systems which are operated on land, sea and airborne platforms in many countries worldwide. The JTIDS and MIDS produce the same waveform and are the radio terminals for transmission of Link 16. The waveform is a hybrid direct sequence and frequency hopping spread-spectrum system that operates on 51 different carrier frequencies in the frequency bands of 969 – 1008 MHz, 1053 – 1065 MHz and 1113 – 1206 MHz. It operates on frequency channels in the region surrounding and including the GPS/Galileo L5/E5a frequency band. A remap capability has been implemented where it would have the capability to operate on as few as 37 carrier frequencies, which could result in added pulse density within the L5/E5a band when compared to the 51 carrier case.

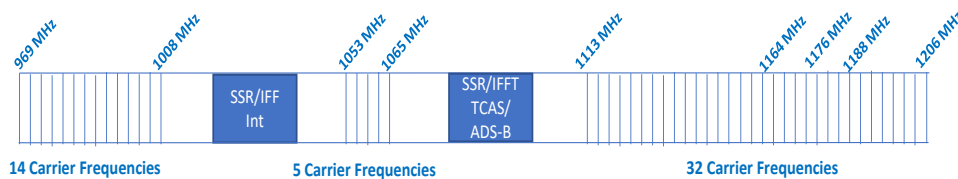


Fig. 1. JTIDS/MIDS Carrier Frequencies

These pulsed signals will then propagate to the aircraft receiver antenna and will then superimpose to thermal noise and to the other received signals, nominally from the useful GNSS satellite, and from the other GNSS satellites.

The receiver considered in our study includes a temporal blanker as described in paper [3]. This temporal blanker is typically modeled as a detector making a decision on zeroing ADC samples based on the comparison of an estimated sampled signal power over a  $1 \mu\text{s}$  window to a blanking threshold. As shown in [3], the optimum blanking threshold selected by the Rx designers can vary by 1 or 2 dBs around the optimal value of  $B_{TH} = -120\text{dBW}$  or  $B_{TH} = -121\text{dBW}$ . It has been shown that  $B_{TH} = -121\text{dBW}$  is better suited to cope with JTIDS/MIDS scenarios such as original Case VIII scenario.

### 1.A) Generic airborne civil aviation GNSS receiver

In order to understand the  $C/N_0$  degradation analytical model, a generic airborne civil aviation GNSS receiver structure as well as the behavior and effect of its components on the received signals are described. The receiver structure is presented here.

First, the antenna is the element responsible of capturing the incoming electro-magnetic waves with modulated signal: at the antenna port, there is a mix of all incoming signals; useful signals, GNSS and SBAS signals, and RFI signals such as DME/TACAN, JTIDS/MIDS, etc. Once the signals have been captured by the antenna, they are passed to the Radio-Frequency Front-End (RFFE) block. This block amplifies the received signals, shifts or down-converts them from their received signal frequency carrier to the intermediate frequency and filters them (removing the image frequency, the spurious frequencies as well as the signal outside the frequency bandwidth of interest). RTCA DO-292 [1] defines the joint effect of these two filters plus the antenna filtering effect with an equivalent filter transfer function; the equivalent transfer function,  $H_{RF}(f)$ , for a 20MHz filter bandwidth is provided in [1].

The RFFE block is also responsible for gain control and digitizing the filtered signals with the application first of the AGC (Automatic Gain Control) circuit followed by ADC (Analog-Digital-Converter). In the case of the proposed airborne civil aviation L5/E5a GNSS receiver after the RFFE block, the digital pulse blanker is introduced. As explained in the introduction, the blanker is a device which is going to blank (put to 0s) the time and/or frequency samples of the incoming signal (mix of signals) that exceed a set threshold. In RTCA DO-292 [1], the defined blanker is a temporal blanker called an “instantaneous blanker”. This blanking mechanism removes all the incoming signal time samples which have a power over a given threshold (issues concerning its actual description and physical implementation are addressed in [3]). For an optimal functioning, the blanker should also be coupled with the AGC/ADC blocks: to ensure that high-power pulses are not saturating the AGC/ADC and that the blanked signal spans the ADC quantization range. The effect of the AGC/ADC and its coupling with the blanker are out of scope of this paper. The digitized and post blanker signals are fed to the correlator. Finally, the RFI signals at the correlator output is where the demodulation, acquisition and tracking capabilities of the receiver can be impacted. It is at this point that these impacts are predicted and simulated within the analysis in this paper.

### 1.B) General analytical model

The key figure of merit to analyze the RFI signals and the blanking method impact is the signal  $C/N_0$  degradation or more specifically, the difference between the  $C/N_0$  when only the useful signal is present at the receiver antenna port (no RFI signals) and the  $C/N_0$  when the useful signal and RFI signals are present at the receiver antenna port (with blanker activation); the latter  $C/N_0$  is also called effective  $C/N_0$  or  $C/N_{0,eff}$ .

Although the blanking method is going to reduce the average power of the useful signal (part of the information signal is removed as well as the noise power), RTCA DO-292 [1] recommended to model the  $C/N_{0,eff}$  by defining an equivalent  $N_{0,eff}$  while keeping the original useful signal power,  $C$ . Note that  $N_{0,eff}$  represents the effective noise power spectrum density that a receiver will observe at the correlator output if the receiver captures a useful signal with power  $C$  at the correlator output. This assumes that subsequent RFFE elements are considered as ideal (RF filter, IF filter, AGC/ADC), the correlator is also considered ideal, there are no RFI signals present and the blanker is not activated. In other words, in section 2.6.2.3, RTCA DO-292 [1] recommended a generic formula to compute the degradation of the  $C/N_0$  through the increase of the background noise due to pulsed and continuous RFI, based on rigorous evaluation within the RTCA Special Committee 159.

In order to mathematically model  $N_{0,eff}$ , the following concepts about the blanking and the incoming signals must be considered. Firstly, although all received L5/E5a GNSS and SBAS signals are by definition useful signals, the receiver has to isolate the signals one-by-one to exploit them. The GNSS and SBAS signals which are not tackled by a specific channel (correlator) are also considered RFI signals. In other words, if the receiver is trying to isolate a GNSS (or SBAS) signal  $i$  in one correlator block, all the other GNSS (or SBAS) signals  $j$ ,  $j \neq i$ , falling in the L5/E5a band are considered RFI signals. These signals are continuous (non-pulsed) signals and its contribution is modelled with the term  $I_{0,WB}$ . Note that the blanking method will not target these signals since they are continuous and thus, the blanking method settings will be determined by the pulsed RFI signals, such as DME/TACAN and JTIDS/MIDS. It is important to realize that a blanker threshold must be chosen high enough above the thermal noise and the continuous signal  $I_{0,WB}$  to avoid receiver excessive blanking of the useful signal effectively saturating the receiver. Secondly, pulsed RFI signals impacts in two different ways  $C/N_{0,eff}$ :

1) Part of the signal is removed due to the blanking and since the impact on the removed useful signal power,  $(1-bdc)^2$ , is higher than the impact on the power of the noise,  $(1-bdc)$ , the equivalent  $N_{0,eff}$  can be seen to be increased by a factor of  $1/(1-bdc)$ . The acronym  $bdc$  represents the blanker duty cycle, or in other words, the percentage of time the incoming useful signal is blanked ( $bdc \in [0,1]$ ).

2) Not all the RFI signal samples have a power above the threshold; therefore, there is a part of the RFI signal that is not removed and its influence must be added to the thermal noise;  $R_I$  is the below-threshold interfering-signal-to-thermal-noise ratio.

From these considerations,  $N_{0,eff}$  can be modelled as:

$$N_{0,eff} = \frac{N_0}{1-bdc} * \left(1 + \frac{I_{0,WB}}{N_0} + R_I\right) \quad (1)$$

$$R_I = \sum_{i=1}^I R_{I,i} \quad (2)$$

Where  $I$  is the total number of pulsed RFI signals,  $R_{I,i}$  is the pulsed source  $i$  below-blanker interfering-signal-to-thermal-noise ratio,  $I_{0,WB}$ , also called the  $I_{GNSS}$ , is the equivalent white noise power spectrum density generated by the continuous interfering signals (in that case only GNSS/SBAS signals are included) at the correlator output.

Finally,  $C/N_0$  degradation can be calculated by comparing  $N_{0,eff}$  to  $N_0$ :

$$Deg = 10 \log_{10} \left(1 + \frac{I_{0,WB}}{N_0} + R_I\right) - 10 \log_{10}(1-bdc) \quad (3)$$

## 2) MODEL FOR $I_{GNSS}$

The interference of concern in this paper is the continuous GNSS interference leading to a contribution called  $I_{GNSS}$  to the  $I_{0,WB}$  mentioned above, due to the inter- and intra- GNSS system interference which is a type of continuous interference, that has a received power level so low that it never triggers the blanker. Following Eq (1) above, equivalent white noise PSD created by all GNSS systems interfering with the signal of interest can be decomposed into:

$$I_{gnss} = \frac{1}{\beta_0} \sum_{\text{all signals } j} P_j \times \int_{-\infty}^{+\infty} |H_{RF}(f)|^2 S_{GNSS,j}(f) \times S_{c_m}(f) df$$

From this, we then have:

$$I_{gnss} = \frac{1}{\beta_0} \sum_{\text{all signals } j} P_j \times \int_{-\infty}^{+\infty} |H_{RF}(f)|^2 S_{GNSS,j}(f) \times S_{c_m}(f) df$$

where

- $H_{RF}$  is the RF front-end filter transfer function
- $\beta_k = \int_{-\infty}^{+\infty} |H_{RF}(f)|^2 S_{BB,k}(f) df$  represents the interference power loss due to the RF front-end, ADC (and NOT the blanker) where  $S_{BB,k}$  is the normalized PSD of the interference source  $k$  before the blanker.
- $\beta_0 = \int_{-\infty}^{+\infty} |H_{RF}(f)|^2 S_{c_m}(f) df$  is the GNSS signal power loss due to the RF filter
- $S_{c_m}$  is the unit PSD of the GNSS signal component receiver local replica.
- $S_{GNSS,j}(f)$  is the unit PSD of the interfering GNSS signal component.
- $I_{0,k,cont}$  and  $I_{0,k,pulse}$  are thus the equivalent white noise level created by the continuous and pulsed interference sources

In this case, the Spectral Separation Coefficient (SSC) can be introduced:

$$SSC(c_{s_j}, c_{m_L}, H_{RF_{BB}}) = \int_{-\infty}^{+\infty} |H_{RF}(f)|^2 S_{GNSS,j}(f) \times S_{c_m}(f) df$$

where the coefficient  $c_{s_j}$  is highlighted to represent the modulation of GNSS signal  $j$ .

Let us consider a single GNSS constellation  $S_k$ . The satellites of this constellation might transmit at the same time a plurality of signals in the GNSS band of interest (L1/E1 or L5/E5a). Let us call  $I_{gnss,S_k}$  the resulting equivalent white noise created by constellation  $S_k$ . We can then write:

$$I_{gnss,S_k} = \frac{1}{\beta_0} \sum_{\substack{\text{all} \\ \text{sat} \\ i}} G_{\text{Sat}/\text{User}_i} \sum_{\substack{\text{all} \\ \text{signals} \\ j}} \left( P_{T_{S_k,S_{j,i}}} \int_{-\infty}^{+\infty} |H_{RF}(f)|^2 S_{GNSS,j}(f) \times S_{c_m}(f) df \right)$$

where

- $P_{T_{S_k,S_{j,i}}}$  is the transmitted power of signal j of satellite i
- $G_{\text{Sat}/\text{User}_i}$  is the combined satellite and receiver antenna gain in the direction of Sat<sub>i</sub>

Considering that all satellites transmit their signal j at a power that is below the max power  $P_{T_{S_j,max}}$ , (which is also independent of the satellite) the above expression can be upper-bounded by:

$$I_{gnss,S_k} < I_{gnss,S_k,max}$$

with

$$I_{gnss,S_k,max} = \frac{1}{\beta_0} \left( \underbrace{\sum_{\text{all signals } j} P_{T_{S_j,max}} \times SSC(c_{S_j}, c_{m_L}, H_{RFBB})}_{\text{Aggregate term that can be assessed per system}} \times \underbrace{\sum_{\text{all sat } i} (G_{\text{Sat}_i})}_{\text{Aggregate term that has to be assessed via simulations}} \right)$$

In the above formula, two terms are highlighted:

- The first one, which will be called the maximum aggregate  $I_{SYS}$ , is a term that is constant for a given system assuming that all the satellites of the considered constellations are transmitting the same signals with the same maximum power. This term can be computed based on the knowledge of:
  - The signal modulation
  - The maximum received signal power
  - The received bandwidth
  - The receiver tracking scheme (modulation of the local replica)

All the necessary system information to compute maximum aggregate  $I_{SYS}$  will be given in the paper.

- The second term, referred to as the aggregate antenna gain, represents the total gain that applies to the received signal and accounts for the satellite and receiver antenna gain pattern of all visible satellites. This term thus depends upon the satellite geometry and can be computed based on simulation. To compute this term, it is thus important to have the knowledge of:
  - The satellite constellation
  - The satellite antenna gain
  - The receiver antenna gain

The final value of  $I_{gnss}$  can then be upper-bounded using

$$I_{gnss} < \sum_{\text{Systems } k} I_{gnss,S_k,max}$$

### 3) GNSS SATELLITES AND SIGNALS ASSUMPTIONS

The assumptions on the constellations, signals, and minimum and maximum received power are given in table below.

System	Signal	Modulation	Freq. MHz	Constellation	Tx BW (MHz)	Min Power (dBW)		Max Power (dBW)		Specific Assumption
BDS	B2a data	ACE-BOC(15,10)	1191.795	27 MEO +3 IGSO +5 GEOs	40.92	-156	-153	-148	-145	3 out of 5 GEOs also broadcast SBAS L5
	B2a pilot					X		X		
	B2b data									
	B2b pilot									
	SBAS	BPSK(10)	1176.45	3 GEOs	24	-158		-150.5		
Galileo	E5a data	ALTBOC(15,10)	1191.795	30 MEO	40.92	-	-	-	-	
	E5a pilot					155.75		148.75		
	E5b data					-	152.75	-	145.75	
	E5b pilot					155.75	148.75			
GPS	L5 Data	QPSK(10)	1176.45	30 MEO	30.69	-157.9	-154.9	-150	-147	Large constellation
	L5 Pilot					-157.9		-150		
QZSS	L5 data	QPSK(10)	1176.45	3 HEO + 4 GEO	24.9	-157.9	-154.9	-150	-147	4 GEOs broadcast SBAS L5
	L5 pilot					-157.9		-150		
	L5 SBAS	BPSK(10)				-158		-150.5		
EGNOS	SBAS	BPSK(10)	1176.45	3 GEO	24	-158		-150.5		
WAAS	SBAS	BPSK(10)	1176.45	3 GEO	24	-158		-150.5		
GAGAN	SBAS	BPSK(10)	1176.45	3 GEO	24	-158		-150.5		
SDCM	SBAS	BPSK(10)	1176.45	3 GEO	24	-158		-150.5		
KASS	SBAS	BPSK(10)	1176.45	2 GEO	24	-158		-150.5		
African SBAS1	SBAS	BPSK(10)	1176.45	3 GEO	24	-158		-150.5		
African SBAS2	SBAS	BPSK(10)	1176.45	2 GEO	24	-158		-150.5		
NavIC	SPS	BPSK(1)	1176.45	7 IGSO	24	-159		-154		
	RS	BOC(5,2)			24	-158.5		-150		

For all constellations mentioned above the reference of the data is the SARPs [18] or the draft SARPs, except for QZSS and NAVIC where the reference is the available ICDs.

As explained in the previous section, the computation of the  $I_{GNSS}$  is split in the computation of the maximum aggregate  $I_{SYS}$  and the maximum aggregate antenna gain.

#### 4) COMPUTATION OF THE MAXIMUM AGGREGATE ISYS

The computed maximum aggregate  $I_{SYS}$  can be computed for each system using the summation over all signals transmitted by this system of the SSC and the maximum transmitted power. The SSC for each signal is provided in table below for a local replica which is always a BPSK(10). The resulting maximum aggregate  $I_{SYS}$  is then provided (using the maximum transmitted power in table below) in table below.

$$I_{sys} = \underbrace{\sum_{\text{all signals } j} P_{T_{s_j}, max} \times SSC(c_{s_j}, c_{m_L}, H_{RF_{BB}})}_{\text{Aggregate term that can be assessed per system}}$$

The following table is the table of the spectral separation coefficients for all L5 signals.

Note that this model does not incorporate the  $\beta_0$ , that will further need to be taken into account.

System	Signal	SSC
BDS (assuming ACE-BOC tracked as BPSK)	B2 low data	-74.85
	B2 low pilot	
	B2 high data	
	B2 high pilot	
	SBAS	-71.82
Galileo (assuming ALTBOC tracked as BPSK)	E5a data	-74.84
	E5a pilot	
	E5b data	
	E5b pilot	
GPS	L5 Data	-71.64
	L5 Pilot	
QZSS	L5 data	-71.52
	L5 pilot	
	L5 – SBAS	-71.52
SBAS signals	SBAS	-71.52
IRNSS (assuming BOC tracked as BPSK)	SPS	-70.21
	RS	-74.02

The table below shows the maximum aggregate  $I_{sys}$  for all L5 Signals.

Type of Orbit	System	Maximum Aggregate $I_{sys}$ (dBW/Hz)= $P_{max} * SSC$
Global Systems	BDS	-219.85
	Galileo	-218.52
	GPS	-218.64
	GLONASS	-218.52
Geo-synchronous	BDS – IGSO	-219.85
	QZSS	-219.42
	IRNSS	-221.11
GEO	BDS – GEO with SBAS	-218.52
	BDS – GEO	-219.85
	QZSS GEO	-218.12
	WAAS	-224.05
	EGNOS	-224.05
	MSAS	-224.05
	GAGAN	-224.05
	SDCM	-224.05
KASS	-224.05	

## 5) COMPUTATION OF THE WORST-CASE AGGREGATE ANTENNA GAIN

Now that the maximum aggregate  $I_{SYS}$  has been computed, let us compute the maximum aggregate antenna gain.

The computation of the  $I_{GNSS}$  is done based on the same general methodology as the one performed in Chapter 11 of [1]. There are however certain differences:

The  $I_{GNSS}$  simulations will consider all configurations of Galileo satellites, which means that the intra-system and inter-system interference will be computed based on the same approach and all geometries will be considered to compute the worst-case intra-Galileo interference.

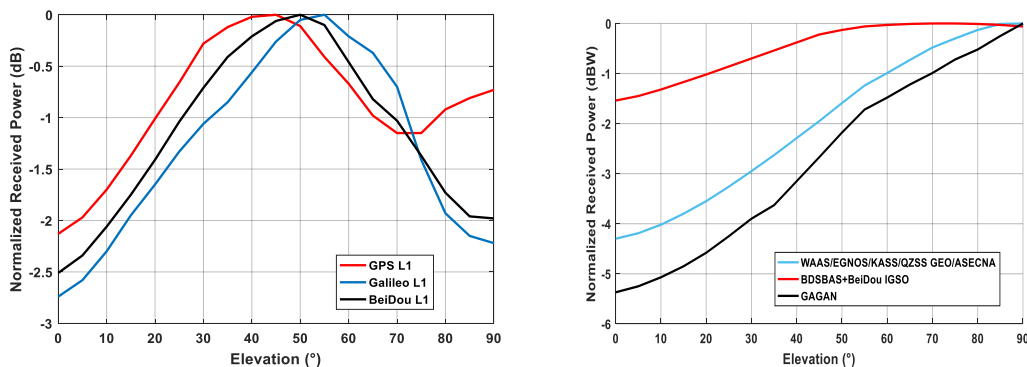
It is assumed that a global constellation will drift over time in the East-West direction with respect to the Earth axis, and that different core constellations will drift with respect to each other. This means that the worst maximum antenna gain created by a given

constellation will be provided only as a function of the latitude. The worst-case aggregate antenna gain per latitude from all global constellations will thus be the sum of the worst contribution of each individual constellation per latitude.

For the regional and SBAS systems, since they are meant to provide a service in a specific well-defined area, it is considered that the associated constellation does not drift in the East-West direction over time with respect to the Earth axis. In this case, the worst contribution of the SBAS and regional systems to the total  $I_{GNSS}$  is computed for each point of a world grid.

To compute the aggregate antenna gain, the simulations must take into account the natural variation of the received power as a function of the relative position of the receiver and the transmitting satellites:

- For satellites that are on a circular orbit, such as the GEOs or MEOs, it is possible to use the received power profile as a function of the satellite elevation. The hypotheses in this case are given in tables above and include GPS, Galileo, BDS, QZSS GEOs and all SBAS except SDCM (see point below for SDCM). In this case, normalized means that the maximum gain over all elevations is equal to 0 dB.
- For satellites that are not on a circular orbit, such as HEOs or IGSOs, or for GEOs that are not pointing towards the center of the Earth, it is then necessary to use the satellite antenna pattern in order to estimate the received power as a function of the relative position of the receiver and the transmitting satellite (only free space losses are considered). The hypothesis in this case are given in tables below and include SDCM and QZSS HEOs. In this case, normalized means that the maximum gain over all elevations is equal to 0 dB. Note that the SDCM pattern is not symmetric since the SDCM antenna is pointing 7° North. The transmitted power then had to be adjusted so that the maximum received gain on the Earth matches the assumption on the maximum received power in table below.



The figure above shows the normalized Received Power vs Elevation (MEO upper, GEO lower).

Note that all computations were done here with antenna gains for L1, assuming that antenna gains for L5 are not larger than the ones for L1. Also, interference environment is dominated by DME/TACAN which makes this difference not critical. The actual computations are made considering the actual L5 gains.

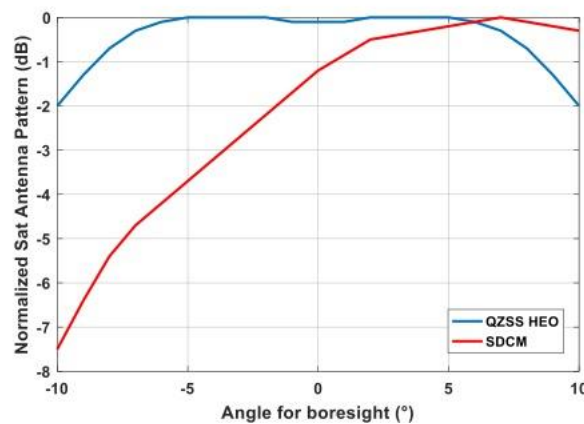
System	Normalized Received Power Pattern vs Elevation	Specific Assumptions
<b>GPS</b>	antenna_elev = [0:5:90]; receivedpower_max = [-2.13 -1.97 -1.70 -1.37 -1.01 -0.66 -0.28 -0.12 -0.02 0 -0.11 -0.41 -0.67 -0.98 -1.15 -1.15 -0.92 -0.81 -0.73];	Improved L1 pattern from Lockheed: [12].
<b>Galileo</b>	antenna_elev = [0:5:90]; receivedpower_max = [-2.74 -2.58 -2.3 -1.95 -1.65 -1.33 -1.06 -0.85 -0.56 -0.26 -0.05 0 -0.21 -0.37 -0.70 -1.41 -1.93 -2.15 -2.22];	Based on IOV satellite antenna pattern: [13].
<b>BDS Phase II+III (MEO)</b>	antenna_elev = [0:5:90]; receivedpower_max = [-2.51 -2.34 -2.06 -1.75 -1.41 -1.04 -0.71 -0.41 -0.21 -0.06 0 -0.10 -0.46 -0.82 -1.03 -1.37 -1.73 -1.96 -1.98];	Based on [14].
<b>All SBAS except SDCM, GAGAN and BDSBAS</b>	antenna_elev = [0:5:90]; receivedpower_max = [-4.30 -4.19 -4.02 -3.80 -3.55 -3.26 -2.95 -2.63 -2.29 -1.95 -1.59 -1.24 -0.99 -0.73 -0.48 -0.30 -0.13 -0.01 0.00];	Based on [15]. Resemblance between WAAS and EGNOS mentioned in [16].
<b>GAGAN</b>	antenna_elev = [0:5:90]; receivedpower_max = [-5.37 -5.25 -5.07 -4.85 -4.58 -4.25 -3.90 -3.63 -3.15 -2.67 -2.18 -1.72 -1.48 -1.22 -0.99 -0.72 -0.52 -0.25 0.00];	Based on [16].
<b>BDS Phase II+III (GEO+IGSO)</b>	antenna_elev = [0:5:90]; receivedpower_max = [-1.54 -1.45 -1.32 -1.17 -1.02 -0.86 -0.70 -0.54 -0.38 -0.22 -0.13 -0.06 -0.03 -0.01 0.00 -0.00 -0.01 -0.03 -0.06];	Based on [14]

Satellite Antenna Gain Assumptions for SDCM and QZSS HEO.

System	Normalized Satellite Antenna Gain Pattern vs Nadir	Specific Assumptions
SDCM	angle = -10:1:10; % negative is south antenna_Txpower = [-7.5 -6.4 -5.4 -4.7 -4.2 -3.7 -3.2 -2.7 -2.2 -1.7 -1.2 -0.85 -0.5 -0.4 -0.3 -0.2 -0.1 0 -0.1 -0.2 -0.3];	SDCM ICD mentions that satellite antenna is pointing 7° North. I think this is a baseline that needs to be taken into account (eg, impact on EGNOS users). Need to use simulations with satellite antenna gain pattern. Satellite antenna pattern deduced from SDCM ICD
QZSS HEO	angle = 0:1:10; antenna_Txpower = [-0.1 -0.1 0.0 0.0 0.0 0.0 -0.1 -0.3 -0.7 -1.3 -2.0];	Because of strong variations of distance for a given elevation angle (HEO orbit), need to use simulations with satellite antenna gain pattern. Satellite antenna pattern deduced from QZSS ICD.

The normalized satellite antenna gain for SDCM and QZSS HEO is shown in the next figure.

Figure 6 2 – Normalized Satellite Antenna Pattern vs Angle from Boresight for L1 (South/North Axis, negative angle means South)



The computation of the aggregate antenna gain for a specific constellation is based on the computation of the satellite elevation angle for each user location, and the summation of the total (satellite/user) antenna gain for all visible satellites. This is done over time and only the largest aggregate gain is kept per location per system.

The computation of the worst-case  $I_{gnss}$  is based on a different consideration of the worst-case MEO and non-MEO (GEO, GEO-synchronous) constellations:

- The MEO satellites are part of a global constellation. The orbital planes of these MEO satellites can rotate over time around the Earth axis in a coherent way without consequences on the intended services. As a consequence, the maximum contribution of the MEO constellations to the  $I_{gnss}$  at a given latitude can be located at any user longitude. In this case, it is necessary to use the following formula to bound per latitude the  $I_{gnss}$  due to global constellations:

$$I_{gnss,global}(latitude) = \sum_{All\ global\ systems} \max_{long} (I_{gnss,S_k}(latitude))$$

where the maximum for a given latitude for a given system is taken over all the longitudes.

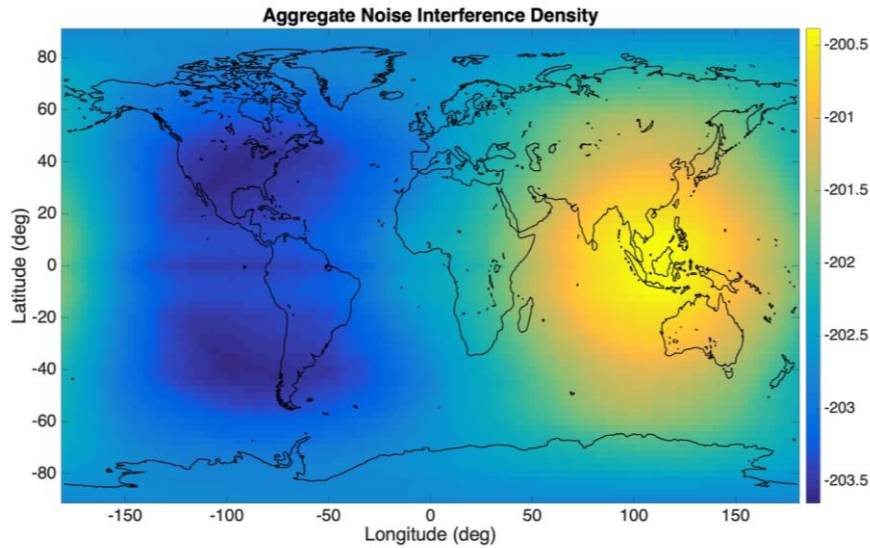
There is thus one  $I_{gnss,global}$  value per latitude.

- The non-MEO satellites are meant to provide a service over a given limited area. It is thus assumed that the satellites' orbits remain on the same orbit over time. In this case, it is thus possible to have  $I_{gnss,regional}$  for any geographical location.

## 6) RESULTS OF $I_{GNSS}$ FOR L5/E5A

The worst-case  $I_{GNSS}$  is then obtained by summing up the  $I_{gnss,regional}$  with  $I_{gnss,global}$  per latitude.

Based on the previous description of the methodology, the worst case  $I_{GNSS}$  as a function of the user location is provided in **Erreur ! Source du renvoi introuvable.** It can be seen that the hot spot is clearly located in South East Asia that is subject to QZSS, BDS GEO and IGSO, GAGAN, NavIC, KASS on top of the global constellations. The resulting evaluation of the  $I_{GNSS}$  leads to the figure below.



The worst case is located at (7.5°N,117.5°E) in South East Asia with a value of -200.38 dBW/Hz for a BPSK10 and BW2=12 MHz Receiver.

Note that this value has to be consolidated as the simulation assumes an average receiver antenna gain pattern similar to the one taken in [2] for the L1  $I_{GNSS}$  assessment. Note also that differently to [2] methodology, no implementation losses are applied to the interfering signals as it is known that they are highly dependent upon the receiver RF front-end configuration (type of ADC, bandwidth, sampling frequency) and the incoming signals. This latter point is already mentioned in the setting of the global degradation model. However, note that the specific RF filter is considered for the computation of the SSC.

The need for a margin in the evaluation of the  $I_{GNSS}$  is coming from the link budget analysis made on L1. Indeed, over the years, the L1 band has seen an increasing number of GNSS systems broadcast new signals, resulting in a difficulty to close the L1 link budget. It thus seems appropriate to anticipate this to cover for potential new future GNSS or GNSS augmentation systems in the L5 band. Simulations were run to consider the possibility of several SBAS service providers using non-GEO satellites to broadcast SBAS L5 signals. The simulation assumes a total of 24 non-GEO satellites, used by 7 SBAS systems. The simulation assumes that these satellites transmit simultaneously with the maximum allowed power introduced in DFMC SBAS SARPs material.

The consideration of the non-GEO SBAS satellites increases the  $I_{GNSS}$  compared to the nominal case by 0.2 to 0.8 dB depending upon the location of the user. Considering that the use of 24 SBAS L5 non-GEO satellites might appear quite pessimistic, it is thus here assumed that a global margin of 0.5dB on the computation of the  $I_{GNSS}$  (without SBAS L5 non-GEO satellites) is adequate.

## CONCLUSIONS

A link budget analysis will be performed for all systems considered (GPS, Galileo, SBAS) based on different limiting scenarios (high altitude, transition altitude, low altitude). The link budget analysis will be performed using the latest available DME/TACAN databases in Europe and USA, as well as the worst case scenarios for JTIDS/MIDS transmission.

It will also include the max  $I_{GNSS}$  presented above to derive the efficient  $N_0$  as given by equation (1) in this paper.

The above-mentioned link budget analysis with the elements considered above should show positive margins (in terms of worst-case C/N0 versus threshold). These margins will be considered as representative of the maximum amount of aggregate continuous interference tolerable coming from non-aeronautical systems (besides JTIDS/MIDS). As a consequence, the smallest margin of all the link budget analysis will be representative of the most fragile link and will thus be the base for the definition of the L5/E5a interference mask.

## ACKNOWLEDGEMENTS

Dr. Olivier JULIEN's work contributing to this paper was exclusively performed when he was ENAC employee.

## REFERENCES

- [1] RTCA, DO 292 - Assessment of RF interference relevant to the GNSS L5-E5a band, July 29, 2004
- [2] RTCA, DO 235B - Assessment of RF interference relevant to the GNSS L1 frequency band, March 13, 2008
- [3] A.Garcia-Pena et al., "Efficient DME/TACAN Blanking Method for GNSS-based Navigation in Civil Aviation," Proceedings of the 32nd International Technical Meeting of The Satellite Division of The Institute of Navigation (ION GNSS+ 2019), Miami, Florida, September 2019, pp. 1438-1452.
- [4] A.Garcia-Pena et al., "GNSS C/N0 Degradation Model in Presence of Continuous Wave and Pulsed Interference" Proceedings of the 2020 International Technical Meeting of The Institute of Navigation, Reston, San Diego, January 2020.
- [5] Gao, G. X., Heng, L., Hornbostel, A., Denks, H., Meurer, M., Walter, T., & Enge, P. (2013). "DME/TACAN Interference Mitigation for GNSS: Algorithms and Flight Test Results". *GPS Solutions*, 17(4), 561-573
- [6] Grabowski, J., & Hegarty, C. (2002). "Characterization of L5 Receiver Performance Using Digital Pulse Blanking". Proceedings of the Institute of Navigation GPS, (pp. 1630-1635). Portland, OR.
- [7] Hegarty, C., Van Dierendonck, A. J., Boby, D., & Grabowski, M. T. (2000). "Suppression of Pulsed Interference through Blanking". Proceedings of the IAIN World Congress and the 56th Annual Meeting of The Institute of Navigation , (pp. 399 - 408). San Diego, CA.
- [8] Shallberg, K., Flake, J., Baraban, D., & Hegarty, C. (2018). "Updated Aviation Assessment of Interference in the L5/E5A Bands from Distance Measuring Equipment". Proceedings of the 31st International Technical Meeting of The Satellite Division of the Institute of Navigation (ION GNSS+ 2018), (pp. 1324-1337). Miami, Florida.
- [9] T. Kim and J. Grabowski. "Validation of GPS L5 Coexistence with DME/TACAN and Link-16 Systems," Proceedings of the 16th International Technical Meeting of the Satellite Division of The Institute of Navigation (ION GPS/GNSS 2003), Portland, OR, September 2003, pp. 1455-1469.
- [10] Musumeci, L., Samson, J., & Dovis, F. (2012). Experimental Assessment of Distance Measuring Equipment and Tactical Air Navigation Interference on GPS L5 and Galileo E5a Frequency Bands. 2012 6th ESA Workshop on Satellite Navigation Technologies (Navitec 2012) & European Workshop on GNSS Signals and Signal Processing, (pp. 1-8). Noordwijk. doi:10.1109/NAVITEC.2012.6423064.
- [11] Proakis J.G. and Salehi M., "Digital Communications – 5th Edition", McGrawhill International Edition, 2008
- [12] Marquis WA, Reigh DL (2015) The GPS block IIR and IIR-M broadcast L-band antenna panel: Its Pattern and Performance. *Navigation*, 62, 329-347
- [13] Monjas, F., A. Montesano, C. Montesano, J. J. Llorente, L. E. Cuesta, M. Naranjo, S. A. Arenas, I. Madrazo, L. Martinez, Test Campaign of the IOV (In Orbit Validation) Galileo System Navigation Antenna for Global Positioning, 2010 Proceedings of the Fourth European Conference on Antennas and Propagation (EuCAP)
- [14] Chang X, Mei X, Yang DH (2015) Space Service Volume performance of BDS. 10th ICG— UNOOSA.
- [15] Bean, K., C. Hegarty, D. O'Laughlin, SBAS Intersystem Interference Update, RTCA SC 159 Meeting, March 2016
- [16] Kahr, Erin, Montenbruck, Oliver, O'Keefe, Kyle, "An Analysis of SBAS Signal Reception in Spac", NAVIGATION, Journal of The Institute of Navigation, Vol. 63, No. 3, Fall 2016, pp. 321-333.
- [17] ICAO, Annex 10 to the Convention on International Civil Aviation, Aeronautical Telecommunications, Volume 1, Radio Navigation Aids, 7<sup>th</sup> Edition, July 2018, Amdt 91